Available online at www.sciencedirect.com

ScienceDirect

journal homepage: http://www.elsevier.com/locate/acme

Original Research Article

Correlation between Lüders band formation and precipitation kinetics behaviour during the industrial processing of interstitial free high strength steels

Gurpreet Singh [a], *Tarun Nanda* [a,*], *Sk. Jabed Miadad* [b], *Nemai Chandra Gorain* [c], *T. Venugopalan* [c], *B. Ravi Kumar* [d]

[a] *Mechanical Engineering Department, Thapar Institute of Engineering and Technology, Patiala 147004, India*
[b] *Tata Motors Ltd., Jamshedpur 831010, India*
[c] *Tata Steels Limited, Jamshedpur 831001, India*
[d] *CSIR-National Metallurgical Laboratory, Jamshedpur 831007, India*

ARTICLE INFO

Article history:
Received 19 September 2018
Accepted 22 December 2018
Available online 4 January 2019

Keywords:
IFHS-steels
IF-steels
Lüders band
Batch-annealing
Continuous-annealing

ABSTRACT

Lüders band formation in steels is critical to surface finish during automobile panel manufacturing. This research reports on the problem of Lüders band formation in interstitial free high strength steel compositions (IFHS-steels). The study investigates the effect of chemical composition and processing parameters on the formation of Lüders bands in IFHS-steels. It correlates the problem of Lüders band formation with precipitation kinetics behaviour during the industrial processing of IFHS-steels. Four different compositions viz. Ti-stabilized, Ti-Nb stabilized, low Ti-low Nb, and high Ti-low Nb with high Al were investigated. Annealing parameters were similar to industrial practice followed for batch and continuous annealing lines in steel manufacturing plants. Stabilized IFHS-steel compositions possessing excess of stabilizing elements (Ti, Nb, etc.) for stabilization of interstitial elements (C, N) also showed the problem of Lüders band formation. The new type of IFHS composition containing high Al, investigated in this research, showed no Lüders band formation during batch annealing cycles along with adequate mechanical properties (YS: 190–202 MPa; Δr-value : 1.57; Δr-value: 0.25). Thus, steel compositions with high Al content processed through batch annealing cycle offer a practical solution to the problem of Lüders band formation in IFHS-steels.

* *Corresponding author.*
E-mail address: tarunnanda@thapar.edu (T. Nanda).
https://doi.org/10.1016/j.acme.2018.12.009

1. Introduction

Interstitial-free (IF-steels) and interstitial-free high strength steel sheets (IFHS-steels) of thickness less than 2 mm are extensively utilized for production of various automobile parts, components, and panels [1]. The main applications of IF-steels in automotive industry include fabrication of front and rear door inners, spare wheel well, rear floor pan, etc. [2]. IF-steels consist of extremely small concentration of interstitial atoms, typically <0.003% carbon and <0.004% nitrogen [2]. Addition of titanium (Ti) and/or niobium (Nb) which are carbide/nitride forming elements makes the steel matrix free from interstitial atoms [3]. These steels offer high resistance to thinning due to their high value of Lankford parameter (*r*-value) [4]. These steel grades are produced through cold rolling followed by annealing route. Titanium and/or niobium are added to IF-steels to fix interstitial carbon and/or nitrogen atoms as carbides/nitrides during the annealing process. Annealing process influences the precipitation behaviour, texture, and properties which are critical for formability [5]. Qiu et al. [6] reported increase in *r*-value (from 1.49 to 1.95) and decrease in yield strength (from 95 to 82 MPa) with increase in annealing temperature in the range of 730–820 °C. In recent times, IFHS-steels are replacing IF-steels due to their relatively better formability and high strength. Solid solution strengthening is achieved by addition of phosphorous (P) and manganese (Mn) which give adequate strength to IFHS-steels [7]. Ghosh et al. [8] showed that the high content of phosphorous in IFHS-steel resulted in formation of FeTiP precipitates, in addition to the TiN, TiS, and MnS precipitates. Further, Ghosh et al. [9] also reported decrease in intensity of {1 1 1} texture, and thus formability with formation of FeTiP precipitates in IFHS-steel. Alloy composition concurrent with appropriate annealing process parameters plays a critical role in achieving desired properties in IF/IFHS-steels. Jeong et al. [10] reported increase in elongation and decrease in yield strength and tensile strength of a niobium stabilized IF-steel with increase in aluminium content (0.055–0.16 wt.%). Similarly, Kang et al. [11] also showed increase in formability of IFHS-steels with increase in aluminium content in excess of 0.10 wt.%.

Yield point elongation (YPE) is a well established phenomenon in low carbon steels. When a low carbon steel is strained under tensile deformation, a well defined sharp yield point is observed, followed by an abrupt drop in stress, and then an increase in strain at constant stress. This increase in strain value at a constant stress is known as yield point elongation or Lüders bandformation phenomenon. The presence of Lüders bands on the surface of steel sheet deteriorates the surface finish [12]. Lüders band phenomenonis usually caused by release of dislocations which were locked in Cottrell atmosphere (atmosphere of solute carbon atoms across dislocations) [13]. YPE or Lüders bandformation in IF-steels and IFHS-steels are not widely reported in literature. Gao et al. [14] reported the correlation between yielding behaviour and Hell–Petch slope (k_y) in high purity iron (containing 11 ppm carbon and 8 ppm nitrogen). The authors reported higher value of k_y in specimen showing discontinuous yielding than that showing continuous yielding. Akama et al. [13] reported discontinuous yielding in IF-steels due to presence of nickel in steel composition. The authors concluded that grain refinement strengthening caused due to nickel addition resulted in discontinuous yielding.

In the present work, the effect of BAF and CAL processes (which are typically followed in steel industry) is investigated on four different IFHS-steel compositions. By using a custom designed annealing simulator, it was possible to simulate the process parameters identical to industrial manufacturing processes. The focus was primarily to investigate the effect of a given annealing route on the efficacy of stabilizing elements present in the given steel compositionto eliminate the formation of undesirable Lüders bands. Finally, the results obtained were verified for a few industrially produced IF/IFHS-steel grades.

2. Materials and methods

Four different IFHS-steel compositionswere used to understand the role of alloying elements viz. titanium (Ti), niobium (Nb), and aluminium (Al) on the stabilization of interstitial elements of carbon (C), nitrogen (N), and sulphur (S) during the annealing process. These compositions included: (i) Ti-stabilized IFHS, (ii) Ti-Nb stabilized IFHS, (iii) low Ti-low Nb IFHS, and (iv) high Ti-low Nb with high Al addedIFHS-steel grades. The steel sheets were finished by cold rolling to a thickness of 0.8 mm. Theses were designated as C1, C2, C3, and C4 compositions, respectively as shown in Table 1.

2.1. *Batch and continuous annealing processes*

Steels of various compositions (C1–C4) were subjected to BAF and CAL routes as per the processing details presented in Fig. 1 and Table 2. These process parameters represent the typical industrial production process parameters for BAF and CAL processes [15,16].

Table 1 – Composition of various IFHS steels along with the calculated minimum alloy addition required for interstitial element stabilization.

	Weight percentage of chemical constituents (wt.%)											
Designation for various steels	C	Mn	P	S	Al	N	Nb	Ti	Min Ti (Stab)	Ti*	Min Nb (Stab)	Nb*
C1	0.0030	0.45	0.046	0.008	0.045	0.0028	–	0.042	0.0335	0.0084	–	–
C2	0.0020	0.62	0.032	0.006	0.035	0.0030	0.016	0.064	0.0272	0.0367	0.0155	0.0005
C3	0.0030	0.51	0.048	0.008	0.060	0.0015	0.020	0.022	0.0291	−0.0071	0.0232	−0.0032
C4	0.0037	0.50	0.031	0.005	0.120	0.0016	0.014	0.064	0.0277	0.0362	0.0286	−0.0146

Min Ti (Stab), Min Nb (Stab): critical amount of Ti and Nb, respectively required for complete stabilization of interstitial elements by annealing.
Ti*, Ni*: excess/deficient amount of Ti and Nb, respectively in any composition required for complete stabilization of interstitial atoms.

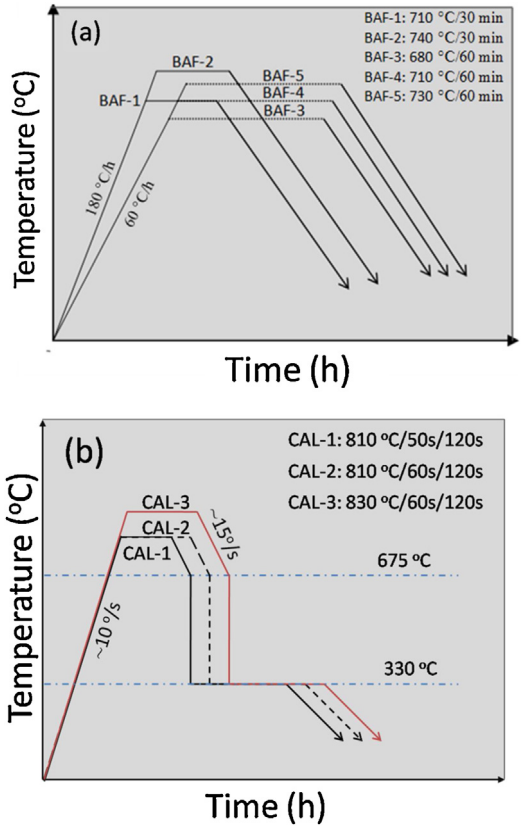

Fig. 1 – Schematic representation of industrial annealing process of (a) batch annealing furnace (BAF) and (b) continuous annealing line process (CAL) used in the present work [15,16].

For C1 and C2 compositions, accelerated BAF processes (BAF-1 and BAF-2) and CAL processes (CAL-1 and CAL-2) were simulated to understand the effect of annealing on interstitial stabilization. In industrial BAF manufacturing process, cold rolled coils, typically of 10–30 tonne each, are stacked one above the other. The stack height is generally of 3–5 coils [17]. Due to the large size and inter-layer air gaps, thermal conductivity is very low in these coils. This causes spatial variation in temperature from outer surface to mid part of the coil. The spatial temperature variation results in microstructure variation at these locations. Therefore, the outer surface is referred to as hot spot and the mid-part as cold spot of the coil during annealing. In view of this spatial variation of temperature, two different peak annealing temperatures were selected in this study to simulate cold (BAF-1) and hot (BAF-2) spot of the coil to capture microstructure variations [18]. Such situations of spatial temperature variations are not encountered in CAL annealing process. However, in CAL process, the effect of variation in soaking period at the annealing temperature was investigated as soaking time affects the Lüders band formation [19]. So, in the present work, CAL-1 and CAL-2 processes were taken which had differences in isothermal annealing time (50 s and 60 s, respectively). BAF simulation duration was about 15 h whereas it was only about 5 min for CAL process. Since C1 and C2 were over-stabilized compositions (contained excess of Ti), it was expected that these compositions can stabilize C easily, and hence accelerated BAF cycles were used for these compositions. As compared to the normal BAF cycle, in accelerated BAF processes, the heating rate (180 °C/s) and annealing temperature were increased (730–740 °C) whereas soaking time (30 min) was decreased [20].

Table 2 – Process parameters for BAF and CAL process.

• Composition: C1 (Ti-stabilized) and C2 (Ti-Nb stabilized) compositions

1. Accelerated BAF simulation

Annealing process	Heating rate (°C/h)	Annealing temperature (°C)	Soaking time (min)
BAF-1	180	710	30
BAF-2	180	740	30

2. CAL process

Annealing process	T1 (°C)	Soaking time (s)	T2 (°C)	Ageing time (s)
CAL-1	810	50	330	120
CAL-2	810	60	330	120

• Composition: C3 (lowTi-lowNb) and C4 (high Ti-low Nb with high Al) compositions

1. BAF industrial simulation

Annealing process	Heating rate (°C/h)	Annealing temperature (°C)	Soaking time (min)
BAF-3	60	680	60
BAF-4	60	710	60
BAF-5	60	730	60

2. CAL process

Annealing process	T1 (°C)	Soaking time (s)	T2 (°C)	Ageing time (s)
CAL-1	810	50	330	120
CAL-2	810	60	330	120
CAL-3	830	60	330	120

Annealing experimentation was performed in a custom designed annealing simulator developed jointly by Tata Steels, Jamshedpur and CSIR-NML, Jamshedpur, India (Fig. 2). Annealing atmosphere comprised of a mixture of 90% N_2 and 10% H_2 gases. Different cooling rates were achieved by varying purging pressure, or volume ratio of '$N_2 + H_2$' gases, or both.

2.2. *Tensile testing*

Tensile specimens (gauge length: 50 mm; width: 12.5 mm) were machined from as-received steel samples as per ASTM standard E-8M. After annealing, samples were tensile tested using an Instron 8862 system of 100 kN capacity (Instron Engg. Inc., Norwood, USA) at a rate of 1 mm/min [21].

2.3. *Characterization for observing precipitaes using SEM/EDS and TEM/EDS*

The precipitates formed in steel during annealing were analyzed using FEG-SEM (FEI NovaNanoSEM 430 SEM system, Field Emission Inc., Hillsboro, USA) and TEM micrographs (JEOL JEM 2200FS TEM, JEOL, USA). For FEG-SEM analysis, sample preparation involved standard metallographic procedure. For TEM analysis, sample preparation was done according to the thin foil method. For this, thickness of annealed samples was reduced from 0.8 mm to 0.06 mm using SiC emery papers. Subsequently, a disc of 3 mm diameter was punched out from the sample. This disc was electro-polished using solution of 10 ml perchloric acid in 90 ml ethanol. Further, the composition of observed precipitates was determined by EDS analysis to correlate Lüders band formation with precipitation behaviour.

2.4. *Formability studies*

Lankford parameter or normal anisotropy (r-value) is a measure of formability/drawability possessed by a steel specimen and signifies its resistance against thinning [22]. Further, planar anisotropy (Δr) is a measure of sheet's tendency to be drawn non-uniformly and represents earing (defect) phenomenon during the forming operation [23]. For calculation of Lankford parameter, initially the plastic strain ratio (r) is defined. According to ASTM E517-00 standard, the plastic strain ratio (r) for uniaxial tensile testing is given as Eq. (1) [24]:

$$r = \frac{\text{true width strain}}{\text{true thickness strain}} = \frac{\epsilon_w}{\epsilon_t} = \frac{\ln(w/w_0)}{\ln(t/t_0)} \tag{1}$$

where w_0 is the initial width, w is the final width, t_0 is the initial thickness, and t is the final thickness. In the present work, the r value (as given by Eq. (1)) was measured in all the three directions viz. rolling direction (r_0), transverse direction (r_{90}) and diagonal direction (r_{45}). Finally, normal anisotropy (Lankford parameter) and planar anisotropy (Δr) were calculated as given by Eqs. (2) and (3), respectively [24]:

$$\text{Normal anisotropy (Lankford parameter)} = \bar{r} = \frac{r_0 = 2r_{45} + r_{90}}{4} \tag{2}$$

$$\text{Planar anisotropy, } \Delta r = \frac{r_0 - 2r_{45} + r_{90}}{2} \tag{3}$$

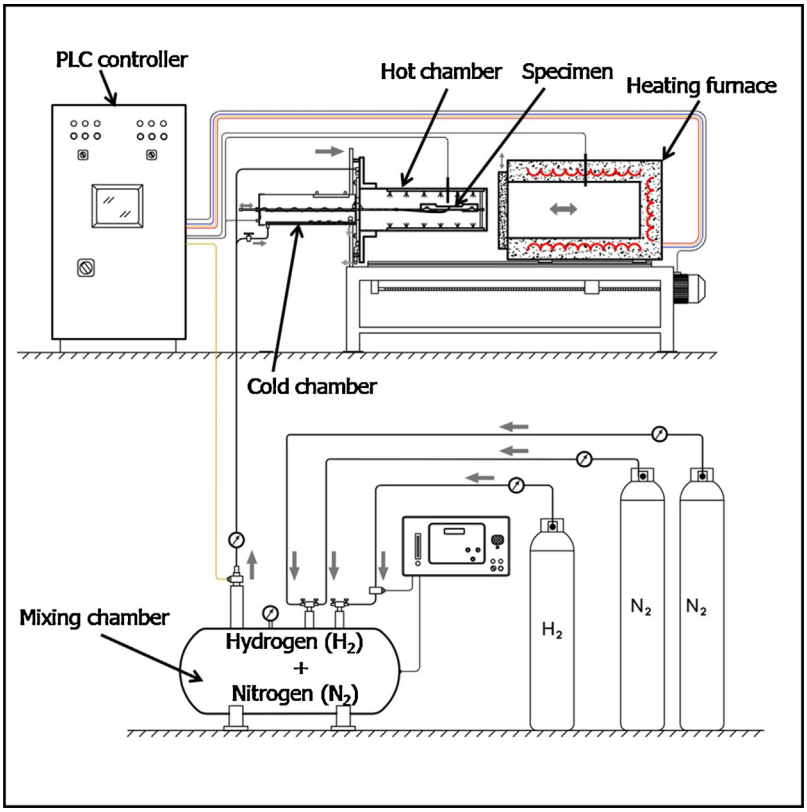

Fig. 2 – Annealing simulator used for processing of steel samples.

3. Results and discussion

3.1. *Effect of annealing processes on stabilization of interstitials elements*

In this study, IFHS-steel compositions were stabilized with Ti and/or Nb alloy additions in varying amounts. The critical amount of Ti and Nb required for achieving complete stabilization of all interstitial elements by annealing process can be estimated empirically as given by Eqs. (4) and (5) [2,19]:

$$\begin{aligned} \mathrm{Ti\ (stab)} &= \frac{48}{14}\mathrm{N} + \frac{48}{32}\mathrm{S} + \frac{48}{12}\mathrm{C} \\ \mathrm{Ti\ (stab)} &= 3.42\mathrm{N} + 1.5\mathrm{S} + 4\mathrm{C} \end{aligned} \tag{4}$$

where Ti, N, S, and C represent the amounts of titanium, nitrogen, suphur, and carbon in wt.%, respectively. The numerals 48, 14, 32, and 12 (all in a.m.u.), signify the atomic weights of titanium, nitrogen, suphur, and carbon, respectively.

$$\begin{aligned} \mathrm{Nb\ (stab)} &= \frac{93}{12}\mathrm{C} \\ \mathrm{Nb\ (stab)} &= 7.75\mathrm{C} \end{aligned} \tag{5}$$

where Nb and C represent the amounts of niobium and carbon in wt.%, respectively. The numerals 93 and 12 (both in a.m.u.), represent the atomic weights of Nb and C, respectively.

When both Ti and Nb are present in steel composition, Ti acts as the main C stabilizer. Nb acts as a stabilizer and/or grain boundary strengthener. Most of the Nb remains in solid solution and only the remaining small proportion of Nb stabilizes C as 'NbC' [5]. Further, the excess/deficient amount of Ti and Nb (referred here as Ti* and Nb*) in any composition required for complete stabilization of interstitial atoms is given as Eqs. (6) and (7) [25]:

$$\mathrm{Ti^{*}} = \mathrm{Ti_{total}} - \mathrm{Ti\ (stab)} \tag{6}$$

$$\mathrm{Nb^{*}} = \mathrm{Nb_{total}} - \mathrm{Nb\ (stab)} \tag{7}$$

$\mathrm{Ti_{total}}$ and $\mathrm{Nb_{total}}$ represent the total amount of titanium and niobium, respectively present in steel chemical composition. A positive value of Ti* (or Nb*) showed that excess amount of Ti (or Nb) was present in steel composition than that was required for complete stabilization of interstitials. Similarly, a negative value of Ti* (or Nb*) showed a deficiency of Ti (or Nb) in the composition.

3.1.1. *C1 composition subjected to annealing process*

C1 was a Ti-stabilized composition in which 0.0084 wt.% of Ti was availablein excess as per Eq. (6) (refer Table 1). Complete stabilization of all interstitial elements was theoretically anticipated for this composition due to presence of Ti in excess.

3.1.1.1. Effect of annealing process on precipitation characteristics. SEM-EDS analysis was conducted for C1 specimensubjected to various annealing processes viz. BAF-1/BAF-2 and CAL-1/CAL-2 (as per Table 2). Various types of precipitates were observed in the microstructure. Fig. 3(a)–(f) shows SEM micrographs along with EDS spectra for one typical annealing process of BAF-2. A large fraction of complex and globular shaped (Ti + Mn)S type precipitates with average size in the range of 0.2–2.0 μm were observed. Further, these precipitates were found to nucleate both at grain interior as well as boundaries. In general, TiN precipitates were observed to form in regular geometrical shapes (i.e. rectangular/square) in size range of 2.0–2.5 μm. It is well reported in literature that for BAF processes conducted near temperatures of 700 °C (for compositions of the type C1), TiS precipitates are formed and subsequently these start converting into MnS precipitates [8]. So Ti, Mn, and S co-exist in the same precipitate showing this conversion and facilitating formation of (Ti + Mn)S, as shown in the present work. Further, a few FeTiP type precipitates (in fine globular shapes of less than 1 μm) were observed along with (Ti + Mn)S precipitates. Interestingly, TiC precipitate formation was not observed in this steel (though, theoretically, TiC formation was strongly anticipated because of presence of excess Ti in C1 composition). The absence of TiC precipitates after annealing could be correlated with FeTiP formation. The precipitation of FeTiP hinders the formation of TiC precipitates (since Ti is tied up by FeTiP formation and its availability for TiC formation remains limited [9]. Also, presence of (Ti + Mn)S precipitates in large fraction indicated that a substantial fraction of available Ti in the steel was consumed by S. Literature also reports that values of solubility product for FeTiP and TiC are very close [9]. Further, it is well reported that formation of FeTiP precipitates in IFHS compositions mainly occurs in the temperature range between 600 and 900 °C [26]. Both BAF and CAL processes carried out in this study fall within this temperature range, and therefore, were expected to enable the undesirable FeTiP precipitation.

3.1.1.2. Lüders band formation. Stress–strain curves obtained for BAF and CAL processed steels are presented in Fig. 4. Irrespective of the type of annealing process used, occurrence of Lüders strain was noticed for C1 composition (see Table 3 for magnitude of Lüders strain). For all the annealing processes, Lüders strain was found to be present in a significant amount (>1%) which could have a deleterious effect on surface finish during sheet forming operation. This indicated that under all annealing conditions, interstitial elements could not be fixed for composition C1, even though this composition contained excess of Ti. The yield strength achieved for C1 composition was in the range of 150–180 MPa which is a reasonably good value for an IFHS grade. However, the presence of Lüders bands in this Ti-stabilized composition will not render it useful for industrial applications. Further, precipitation analysis (see Fig. 3) showed that most of the Ti was tied up withsulfur and phosphorous and was not available in sufficient amount to fix interstitial elements. As a result, Lüders band formation occurred during tensile deformation. This observation was contradictory to the prediction arrived at by using empirical equations viz. Eqs. (4) and (6).

3.1.2. *C2 composition subjected to annealing process*

For C2 composition, BAF and CAL process parameters were similar to what were used for C1 composition (Table 2). C2

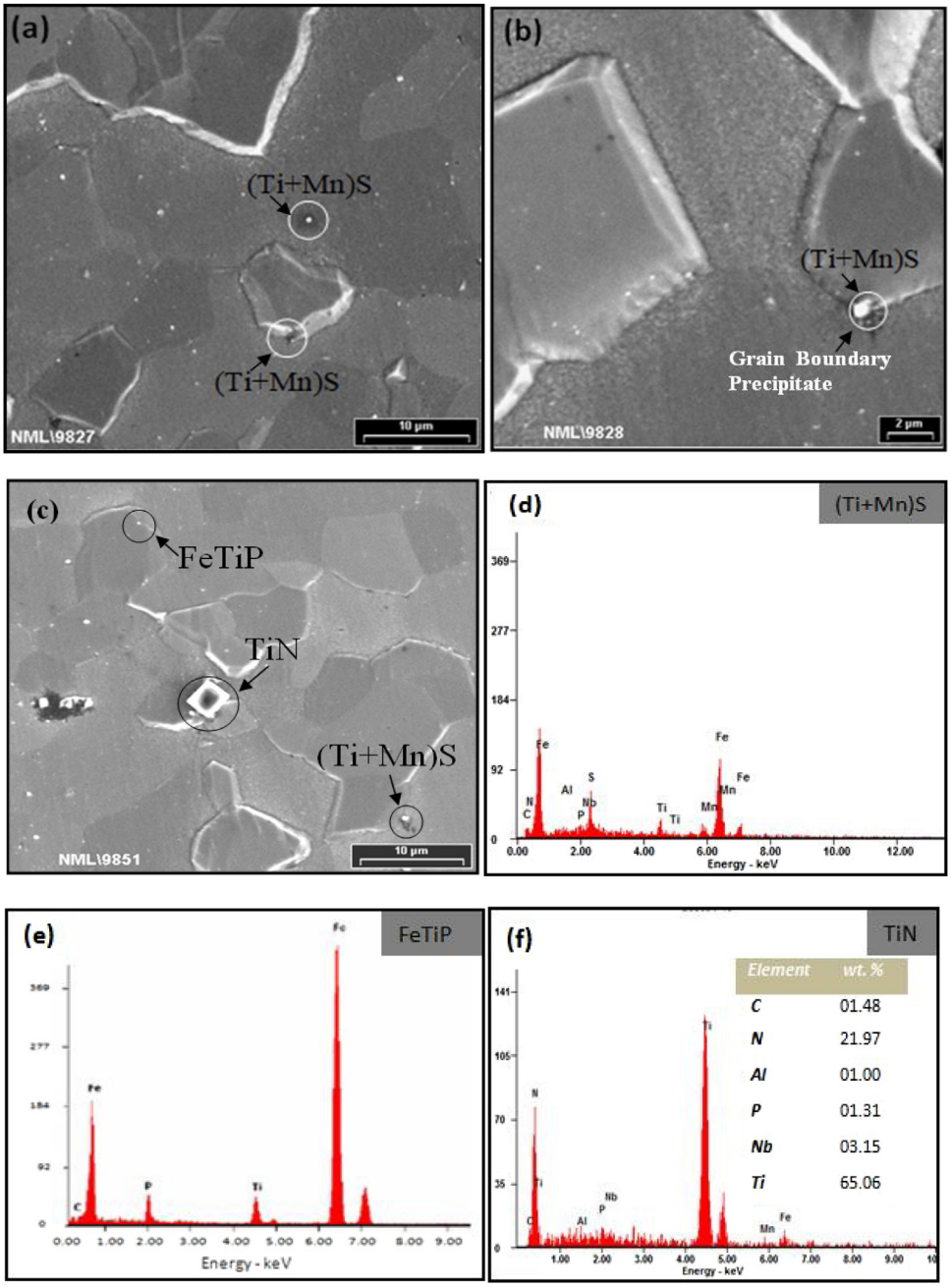

Fig. 3 – SEM micrographs showing (a)–(c) various types of precipitates at grain boundary and also grain interior in C1 specimen subjected to BAF-2 process. (d)–(f) Typical EDS spectra showing the presence of (Ti + Mn)S, FeTiP, and TiN type of precipitates.

composition was Ti stabilized as well as Nb stabilized IFHS-steel in which 0.03671 wt.% of Ti and 0.0005 wt.% of Nb were present in excess as per empirical Eqs. (4)–(7) (Table 1). So, complete stabilization of all interstitial elements was theoretically anticipated for this composition.

3.1.2.1. *Effect of annealing process on precipitation characteristics.* SEM-EDS analysis of C2 specimen subjected to various annealing processes (BAF and CAL processes, Table 2) was carried out which showed formation of various types of precipitates. Fig. 5(a)–(g) shows SEM micrographs/EDS spectra for a typical annealing process of CAL-2 (i.e. annealing at 810 °C with ageing time of 60 s). Precipitates of Ti viz. TiN, TiC, and TiS were observed in high frequency of occurrence and a few precipitates of AlN were also observed as shown in Fig. 5(a)–(d). TiN precipitates were observed in rectangular shape (with average size: 1–3 μm), TiC precipitates in irregular shape (average size: 1–2 μm), TiS precipitates in globular shape (average size: 0.2–1.5 μm), and AlN precipitates in globular shape (average size: 0.2–0.5 μm). However, no precipitates containing Nb were detected by SEM due to the very fine size of such precipitates [27,28]. Precipitates (TiN → TiS → TiC) obtained for Ti-Nb stabilized IFHS-steel (C2 composition) were of the same type as reported in literature [29,30]. For C2

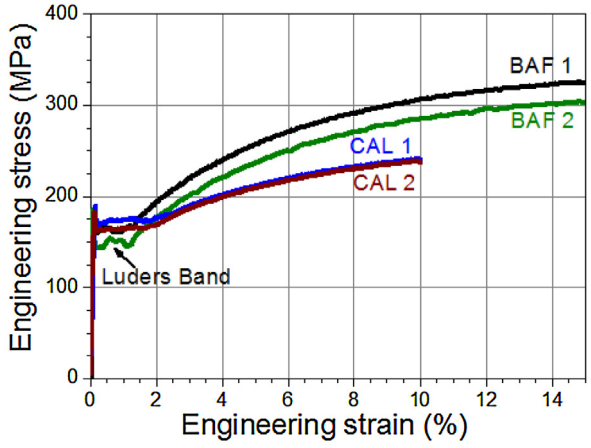

Fig. 4 – Stress–strain curves for C1 composition (Ti-stabilized) for BAF-1, BAF-2, CAL-1, and CAL-2 processes showing formation of Lüders bands.

composition, TiC type precipitates were observed in a significant fraction as shown in Fig. 5(f)–(g). Therefore, the interstitial element carbon present in C2 composition steel appears to be well tied up.

3.1.2.2. Lüders band formation. Stress–strain curves for C2 specimens subjected to BAF and CAL processes (see Fig. 6) did not show any significant yield point elongation/Lüders band formation. Yielding phenomena occurred for less than 0.2% strain for this steel. Lüders bands or stretcher strains adversely affect the surface finish when they are more than 0.3% of yield point elongation [31]. The 0.2% yielding phenomenon was well within the acceptable limits. Therefore, efficient stabilization of major interstitial elements present in the steel led to elimination of Lüders band occurrence. However, despite the absence of Lüders bands, this IFHS composition was not deemed suitable for automotive panel applications because of its low yield strength (125–150 MPa). The main reason for low strength was small amounts of strengthening elements like phosphorous and carbon in this steel. The soluble phosphorous, even in very small amounts (in ferrite matrix), significantly affects the strength of IFHS-steels [32]. Table 3 shows that no Lüders bands and Lüders strain were present in C2 composition indicating suitability of composition for both BAF and CAL annealing processes.

Table 3 – Lüders strain (%) present in IFHS steels subjected to different annealing processes.

Annealing process	C1 composition	C2 composition
BAF-1	1.17	Absent
BAF-2	1.07	Absent
Annealing process	**C1 composition**	**C2 composition**
CAL-1	1.69	Absent
CAL-2	1.41	Absent
Annealing process	**C3 composition**	**C4 composition**
BAF-3	1.48	Absent
BAF-4	1.46	Absent
BAF-5	1.21	Absent
Annealing process	**C3 composition**	**C4 composition**
CAL-1	1.20	Absent
CAL-2	1.00	Absent
CAL-3	–	1.0

3.1.3. C3 composition subjected to annealing process

For C3 composition, BAF processes used were identical to the ones used in industrial practice (very slow heating/cooling rates with total BAF cycle duration of about 24 h) [20,33]. Three different peak annealing temperatures (680, 710, and 730 °C) were used to simulate hot and cold spots conditions of the coil. However, CAL process used for C3 composition was similar to what was used for previous compositions. C3 composition was an under-stabilized composition in which Ti and Nb were available in slightly deficient amounts of −0.0071 and −0.0032 wt.%, respectively as per Eqs. (4)–(7) (see Table 1). From the empirical equation based predictions, only partial stabilization of interstitial elements wasexpected.

3.1.3.1. Effect of annealing process on precipitation characteristics. SEM-EDS analysis of C3 specimens subjected to various annealing processes (as per Table 2) was carried out which showed formation of various types of precipitates (see Fig. 7). Nitrides of Al, Ti, and sulfides of Mn were observed in Fig. 7(a)–(d). The precipitates of AlN were observed to have needle-like shape with a size close to 1.0 μm. Further, precipitates of MnS and TiN were frequently observed together, with sizes in the range of 0.5–1.0 μm. The study showed that N was effectively stabilized by Al and Ti, whereas Mn was mostly tied up with S. However, precipitation of TiC was not observed. The absence of TiC precipitation was attributed to formation of sub-micron FeTiP precipitates. TEM-EDS analysis was used to confirm the presence of FeTiP precipitates because of their very fine size. The results of TEM-EDS analysis confirmed the presence of FeTiP precipitates (average size: 15–25 nm) as shown in Fig. 8(a) and (b). Ghosh et al. [8] also reported that frequency of formation of FeTiP precipitates is more in IFHS-steels containing high phosphorous contents, and in the present work, C3 composition contained highest phosphorous content. Further, C3 composition had low Ti content. Some amount of Ti was taken up by FeTiP precipitate formation (as shown in Fig. 8) and hence effective stabilization of carbon was not possible in this composition, both by BAF and CAL processes.

3.1.3.2. Lüders band formation. The stress–strain curves (see Fig. 9) for various annealing processes for C3 composition showed significant Lüders strain as shown in Table 3. The presence of Lüders strain was to a significant extent (≥1%) which was adequate to cause deterioration of surface finish during forming operation. This composition was not found suitable for BAF/CAL processes in stabilizing carbon. The presence of soluble carbon was responsible for Lüders band formation.

3.1.4. C4 composition subjected to annealing process

For C4 composition, both BAF and CAL annealing processes were used. C4 composition was a stabilized composition

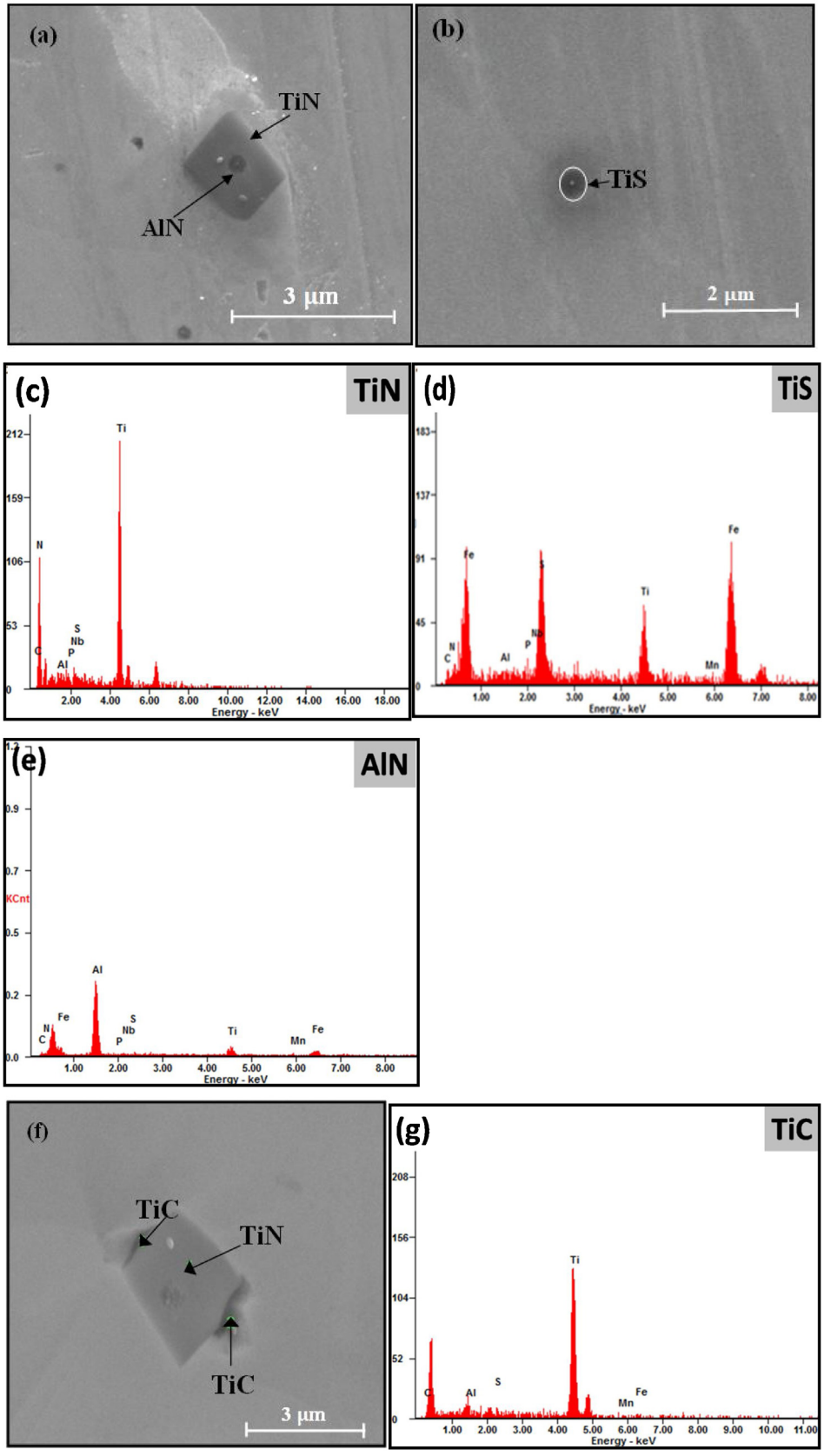

Fig. 5 – SEM micrographs showing (a)–(c) various types of precipitates at grain boundary and grain interior in C2 composition subjected to CAL-2 process. (d)–(f) Typical EDS spectra showing the presence of TiN, TiS, and TiC type of precipitates.

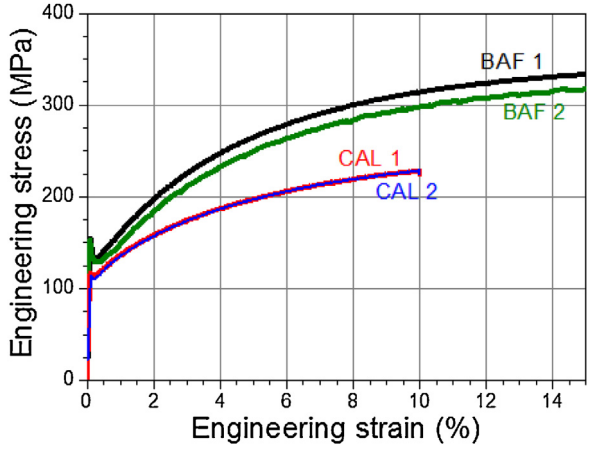

Fig. 6 – Stress–strain curves for C2 composition (Ti-Nb stabilized) for BAF-1, BAF-2, CAL-1, and CAL-2 processes.

containing 0.0362 wt.% of Ti in excess but 0.0146 wt.% of Nb in deficient amount (see Eqs. (4)–(7) and Table 1). Further, it also contained high amount of Al (0.12 wt.%). Jeong et al. [10] reported that addition of Al in IF-steels in amounts greater than 0.10 wt.% results in scavenging of N from the ferrite matrix by formation of coarse AlN precipitates. Further, Kang et al. [11] reported that addition of Al in IFHS-steels in amounts in excess of 0.10 wt.% increases their formability. Due to these advantages of high Al content, C4 composition was investigated. Further, it is also reported in literature that in a given IF-steel composition, if Al amount is more than 0.10% (and further Al/N ratio is significantly greater than the Ti/N ratio), AlN precipitates are formed along with TiN precipitates [34]. Thus, for C4 composition, it was expected that N will be fixed mainly by Al (through formation of AlN) and partially by Ti (through formation of TiN). As a result, it was expected that Ti shall largely remain free for fixing carbon by formation of TiC precipitates.

3.1.4.1. *Effect of annealing process on precipitation characteristics.* SEM-EDS analysis of C4 composition subjected to BAF-3 and BAF-4 processes (as per Table 2) showed presence of various types of precipitates. SEM-EDS analysis revealed that Al addition stabilized the interstitial element N by formation of AlN precipitates. Further, residual N and C elements were mainly stabilized by Ti as TiN and TiC, respectively. Also, S was stabilized by Ti by formation of TiS precipitates. Fig. 10(a)–(i) presents the results of SEM-EDS analysis for one typical BAF process (BAF-3 process at 680 °C) which revealed presence of several AlN, TiC type precipitates and a few TiN and TiS precipitates. AlN precipitates were observed in nearly rectangular/needle type shape (average size: 0.5–5 μm), while those of TiC and TiN were observed in irregular shape (average size: 0.5–5 μm) and square shape (average size: 1.5–5 μm), respectively. Thus, formation of several AlN precipitates and a few TiN precipitates occurred in steel. As a result, Ti was largely available for fixing of C by formation of TiC, thus, locking the soluble C in the ferrite matrix.

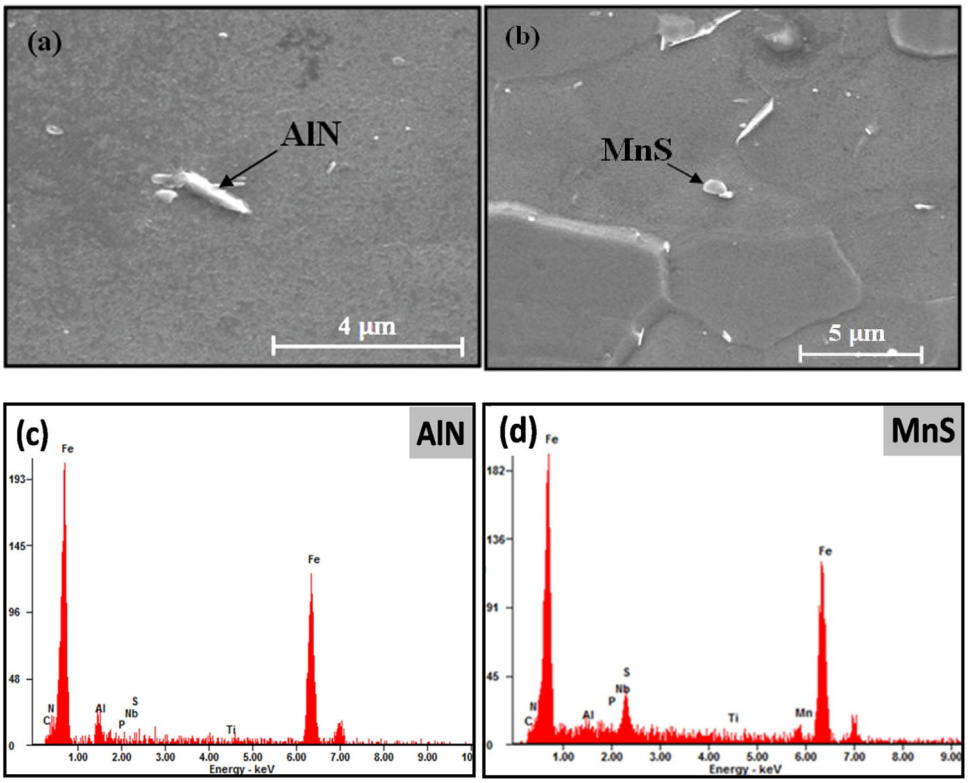

Fig. 7 – SEM micrographs showing various types of precipitates at grain boundary and grain interior in C3 composition subjected to BAF-5 process. (d)–(f) Typical EDS spectra showing the presence of AlN and MnS type of precipitates.

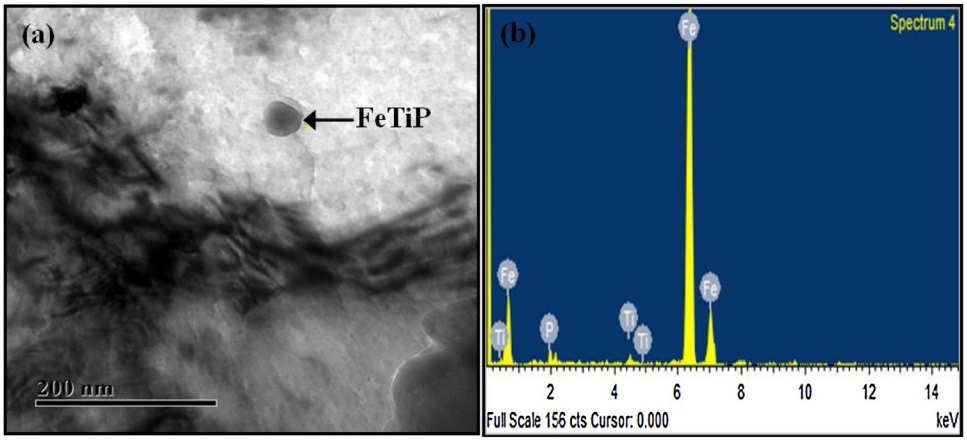

Fig. 8 – (a) Bright field TEM micrograph and (b) EDS spectrum showing FeTiP type precipitates in C3 composition subjected to BAF-5 process.

3.1.4.2. Lüders band formation. The stress–strain curves obtained for C4 composition subjected to various BAF processes did not show Lüders band formation (see Fig. 11 (a) and Table 3). Though yielding phenomena occurred for less than 0.2% strain, but no yield point elongation was present. This indicated that BAF processes for the high aluminium C4 composition were effective in stabilization of interstitial elements (C, N) by means of favourable precipitation kinetics. Further, CAL-1 process (810 °C, 50 s) carried out for C4 composition showed continuous yielding behaviour (see Fig. 11(b)).

Continuous yielding was not expected for C4 composition subjected to CAL-1 annealing route. This is because SEM analysis revealed that AlN precipitates were formed in very low amounts for CAL-1 process. This meant that AlN precipitates started dissolving at this high temperature (810 °C). As AlN was formed in low amounts, the advantage of adding high Al in C4 composition was lost. So, N was mainly tied up by Ti. As a result, less Ti was available for formation of TiC (to tie up C). Thus, from this precipitation kinetics, it was expected that CAL-1 route for C4 composition will lead to discontinuous yielding behaviour. However, since continuous yielding behaviour was shown by C4, it was decided to investigate the microstructure of steel for its recrystallization behaviour. The microstructure of CAL-1 treated C4 steel exhibited incomplete recrystallisationof the cold-rolled structure (see Fig. 12(a)) which was considered responsible for the continuous yielding behaviour. Slower recrystallization kinetics of C4 composition was mainly due to the high Al content present in the composition, as formation of AlN retards the recrystallization phenomena in steels [35]. Further, Cottrell and Bilby [36] reported that discontinuous yielding mainly occurs due to locking of dislocations generated during deformation by the interstitial atoms (i.e. due to formation of Cottrell atmosphere). In the incomplete recrystallised microstructure state wherein dislocations are present in abundance, the efficacy of dislocation locking is generally not adequate by interstitials, resulting in discontinuous yielding behaviour [36]. For obtaining complete recrystallisation, annealing time was increased to 60 s from 50 s (CAL-2). However, despite the increase in annealing time, complete recrystallisation was not achieved (see Fig. 12(b)). Finally, CAL-3 was conducted at a relatively higher temperature (830 °C, 60 s) to accelerate the recrystallisation kinetics. Microstructure observation (Fig. 12(c)) showed complete recrystallisation of the cold rolled structure. However, tensile deformation of CAL-3 processed C4 sample (Fig. 11(b)) indicated incomplete stabilization of interstitial atoms. As discussed earlier, SEM-EDS analysis of CAL-3 processed C4 composition steel showed formation of TiN precipitates in abundance while presence of AlN precipitates was very small.

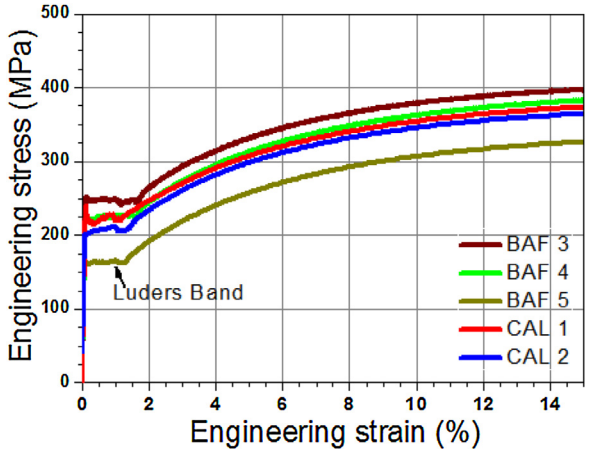

Fig. 9 – Stress–strain curves for C3 composition (low Ti-low Nb) showing occurrence of undesirable Lüders band formation in BAF as well as CAL processes.

Fig. 13 is a typical SEM micrograph for CAL-3 processed C4 specimen. It can be noticed that with increase in annealing temperature to 830 °C in CAL-3 process, the advantage of Al addition in tying up N was lost (AlN precipitates were not observed in SEM micrographs). This had an adverse effect on precipitation kinetics causing a loss in efficacy of Al addition in

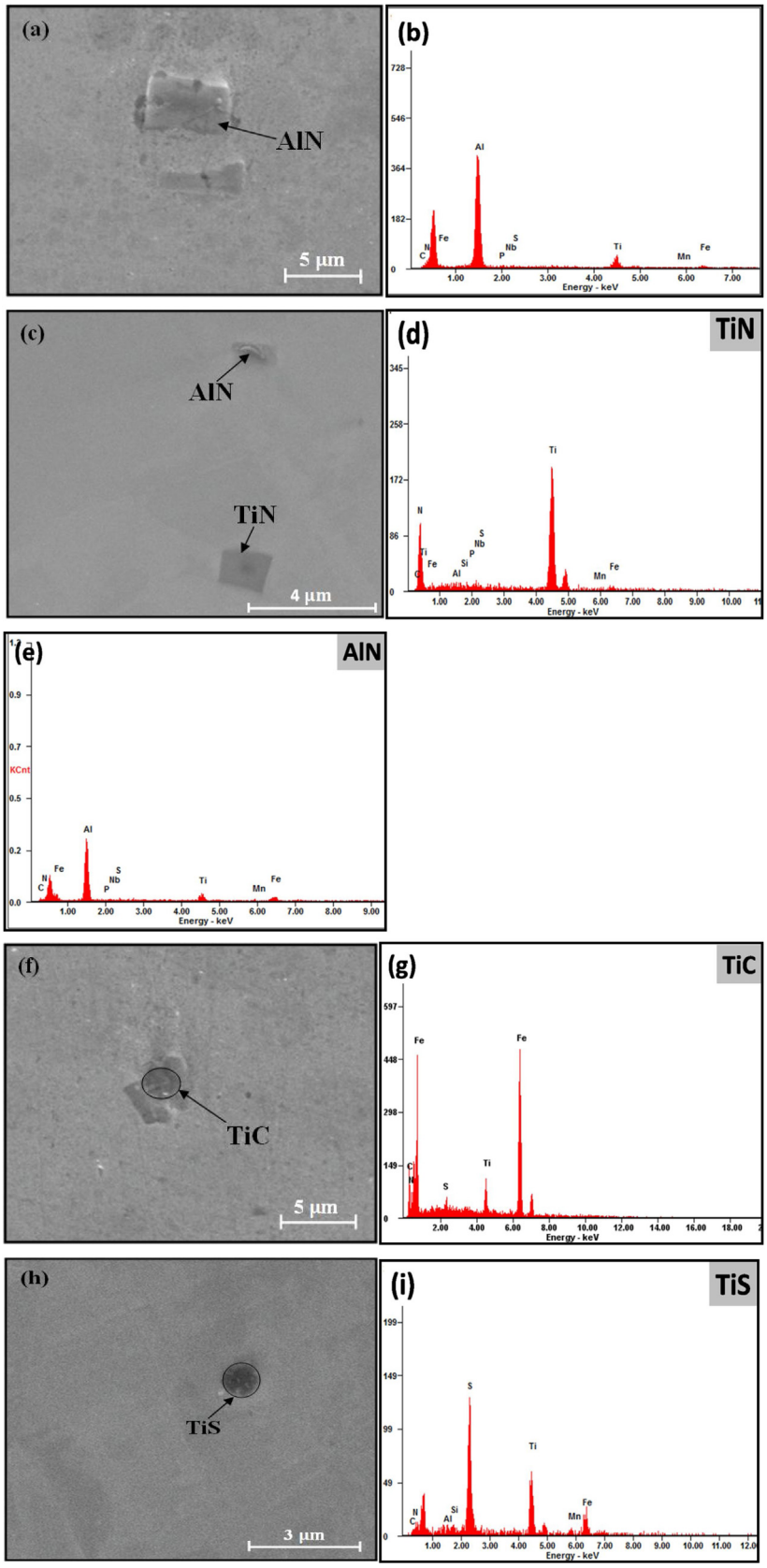

Fig. 10 – SEM microstructures of C4 specimen subjected to BAF-3 process are shown in (a), (c), (f), and (h); EDS spectra showing AlN, TiN, TiC, TiS precipitates in (b), (d), (e), (g), and (i), respectively.

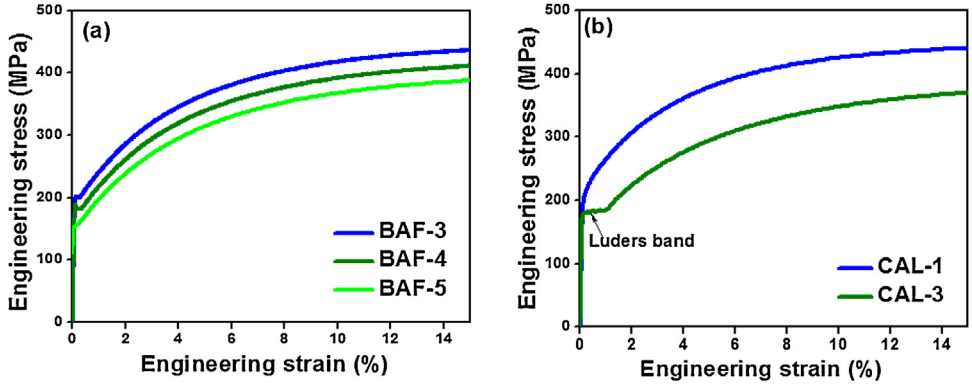

Fig. 11 – Stress–strain curves for C4 composition for (a) BAF-3, BAF-4, BAF-5 processes, and (b) CAL-1, CAL-3* processes. *Formation of undesirable Lüders bands can be noted for CAL-3 process.

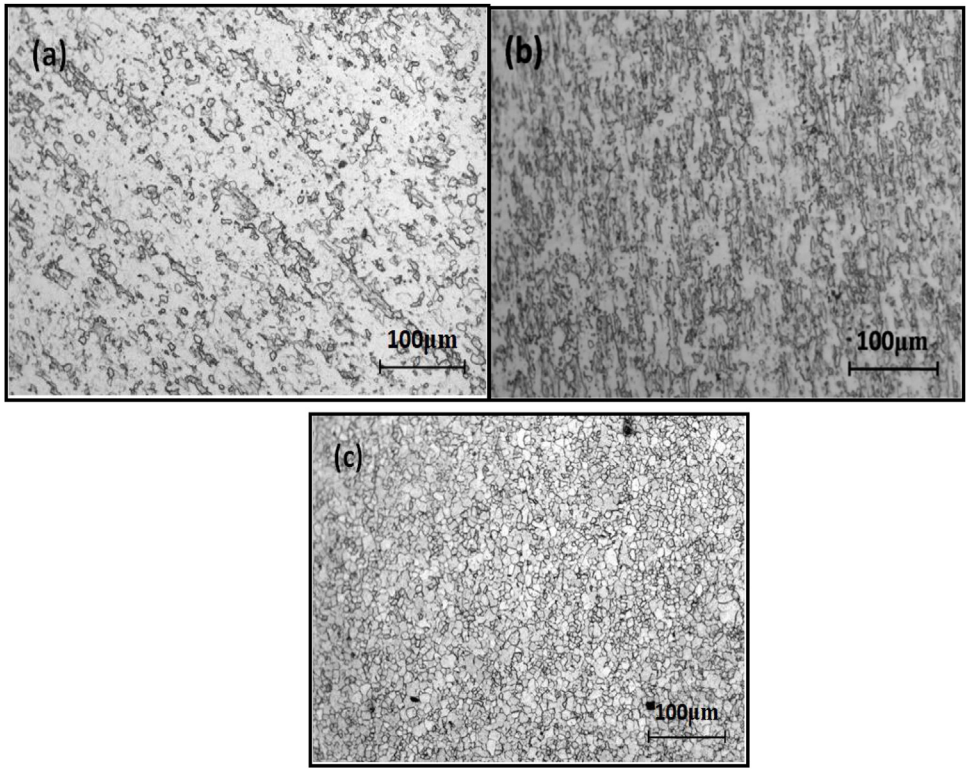

Fig. 12 – Optical micrograph of C4 composition after (a) CAL-1 process (CAL at 810 °C with 50 s soaking) showing incomplete recrystallization, (b) CAL-2 process (CAL at 810 °C with 60 s soaking) showing incomplete recrystallization, and (c) CAL-3 process (CAL at 830 °C with 60 s soaking) showing complete recrystallization. TiN.

consuming N. Ti waslargely consumed in the form of TiN and TiS type precipitates and thus availability of Ti for TiC formation wasreduced (see Fig. 13(a)), which further limited the formation of TiC precipitates. Also, it is reported in literature that at high annealing temperatures (~830 °C), decomposition of NbC in ferrite is also possible which increases the soluble C content in ferrite matrix [26]. All this resulted in incomplete stabilization of carbon, and thus, caused formation of Lüders bands.

The above results showed that C4 composition is useful for industrial production by BAF processes but not by CAL annealing processes. This composition does not provide desirable results in stabilizing the interstitial elements with the industrially used CAL manufacturing process. The mechanical properties of C4 specimens subjected to various BAF processes are shown in Table 4. It can be observed that BAF processes provide a good combination of mechanical properties for C4 composition. The BAF process conducted at a higher

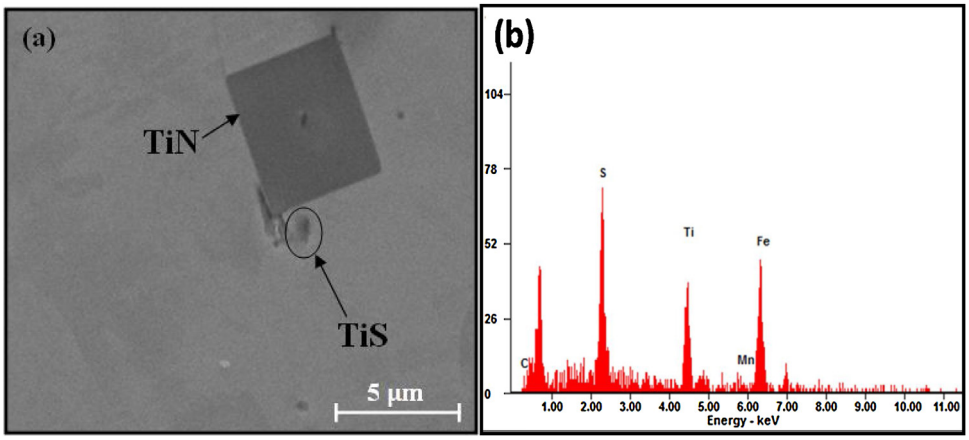

Fig. 13 – (a) SEM microstructure showing occurrence of precipitates of the type TiN, TiS during CAL-3 process and (b) EDS spectrum showing TiS type precipitate analysis.

Table 4 – Mechanical properties obtained in C4 steel specimens after BAF processes.

Batch process	Yield strength (MPa)			r-Value	Δr
	R	T	D		
BAF-3	203	212	204	1.25	−0.27
BAF-4	190	202	197	1.57	0.25
BAF-5	156	167	160	1.95	−0.82

temperature caused a decrease in yield strength but raised the Lankford parameter. BAF-4 process conducted at 710 °C appears to be an optimum process condition for C4 composition, as this process provided the best combination of properties (YS = 190–202 MPa; *r*-value : 1.57; Δ*r*-value = 0.25).

The results obtained in the present research with regards to presence/absence of Lüders bands, precipitation kinetics, and mechanical properties for the four different steel compositions were validated by investigating a few industrially processed steels including: (a) IF-steels (03 compositions), (b) IFHS-steel (01 composition), and (c) high aluminium containing IFHS-steels (03 compostions) processed through BAF and CAL routes. The absence of Lüders bands was considered as the test of stabilization of interstitial elements (see Table 5).

Industrially processed IF-1, IF-2, and IF-3 compositions did not show Lüders band formation. This was in agreement with the reportings of present research where it was stated that because of very low amounts of phosphorous in IF-steels, FeTiP precipitation does not occur, and thus, complete stabilization of interstitial elements occurs.

Next, the industrially BAF processed IFHS composition, refered to as IFHS in Table 5 (similar to the C3 composition evaluated in present work) showed Lüders bands due to FeTiP formation. This was in agreement with the results of present research where BAF processed C3 composition showed Lüders band formation.

Finally, in the present research, Lüders band formation did not occur in the high aluminium C4 composition (Al was in excess of 0.10 wt.%) processed by BAF annealing. In agreement to the results of present research, the industrially used high aluminium IFHS-steels viz. IFHS-Hi Al-1 and IFHS-Hi Al-2 compositions,processed industrially by BAF annealing also did not show Lüders band formation. Further, C4 composition had shown Lüders bands after being processed through CAL route. In a similar manner, the industrially CAL processed IFHS-Hi Al-3 composition also showed Lüders bands formation.

Hence, the results of present research and the industrial data showed complete agreement.

Table 5 – Mechanical properties obtained in some industrially produced steel specimens to validate the results obtained in the present research.

Type of industrially processed steel	Annealing process	Concentration of alloying elements in the steel (wt.%)								r-Value	YS (MPa)	Ti*	Nb*	FeTiP formation	Lüders bands
		C	Mn	P	S	Al	N	Nb	Ti						
IF-1	CAL	0.002	0.10	0.01	0.01	0.05	0.002	0	0.06	1.9	160	0.03	–	No	**No**
IF-2	BAF	0.002	0.10	0.01	0.01	0.06	0.002	0	0.06	1.92	155	0.03	–	No	**No**
IF-3	CAL	0.002	0.10	0.01	0.01	0.03	0.002	0.01	0.03	1.7	167	0.0016	0	No	**No**
IFHS	BAF	0.003	0.50	0.05	0.01	0.04	0.002	0.025	0.04	1.7	212	0.006	0.005	Yes	**Yes**
IFHS-Hi Al-1	BAF	0.002	0.10	0.05	0.01	**0.20**	0.002	0.01	0.03	1.8	189	0.0016	0	No	**No**
IFHS-Hi Al-2	BAF	0.002	0.50	0.05	0.01	**0.10**	0.002	0.02	0.03	1.8	199	0.0016	0.01	No	**No**
IFHS-Hi Al-3	CAL	0.002	0.10	0.05	0.01	**0.20**	0.002	0	0.05	1.85	180	0.0201	−0.01	Yes	**Yes**

The bold ones shows high Al amount present in last three compositions. Bold shows the uniqueness of these compositions.

4. Conclusions

The present research work was an attempt to understand the influence of stabilizing elements viz. Ti and Nb on the selection of industrially used annealing process routes (BAF and CAL) for the production of IFHS-steels. The main conclusions are as follows:

- Selection of a particular annealing route (BAF or CAL) for industrial processing of IFHS-steels depends on the chemical composition of the starting material. The amount of stabilizing elements (Ti, Nb, and Al) present in steel chemistry decide the annealing process parameters. Further, the formation/absence of Lüders bands in steel is strongly dependent on the precipitation behaviour of steel. Deficiency in concentration of stabilizing elements is mainly responsible for Lüders elongation.
- Presence of aluminium as a stabilizing element in steel chemistry shows a significant influence on precipitation behaviour and mechanical properties of the processed IFHS-steels. High aluminium content results in preferential formation of AlN precipitates over TiN precipitates when annealed through the BAF process route. Therefore, for the BAF process, availability of titanium in steel is increased for stabilizing of interstitial carbon.
- For the CAL process, higher annealing temperatures and faster cooling rates as compared to BAF process, increase the concentration of soluble carbon by way of loss of titanium as it ties up with N and by dissociation of NbC in ferrite at high annealing temperatures. To fix this free or dissolved carbon, additional micro-alloying is necessary for effective locking of dislocations during deformation.

Acknowledgments

Authors are thankful to Director, CSIR-National Metallurgical Laboratory, Jamshedpur, for supporting this research and also to the Management of Tata Steels, Jamshedpur for corroborating the research findings of this work with plant production.

REFERENCES

[1] S.K. Paul, Effect of anisotropy on ratcheting: an experimental investigation on IFHS steel sheet, Mater. Sci. Eng. A 538 (2012) 349–355.
[2] S. Hoile, Processing and properties of mild interstitial free steels, Mater. Sci. Technol. 16 (10) (2000) 1079–1093.
[3] S. Carabajar, J. Merlin, V. Massardier, S. Chabanet, Precipitation evolution during the annealing of an interstitial-free steel, Mater. Sci. Eng. A 281 (1–2) (2000) 132–142.
[4] D. Verma, N.K. Mukhopadhyay, G.V. Sastry, R. Manna, Microstructure and mechanical properties of ultrafine-grained interstitial-free steel processed by ECAP, Trans. Indian Inst. Met. 70 (4) (2017) 917–926.
[5] R.K. Ray, P. Ghosh, D. Bhattacharjee, Effects of composition and processing parameters on precipitation and texture formation in microalloyed interstitial free high strength (IFHS) steels, Mater. Sci. Technol. 25 (9) (2009) 1154–1167.
[6] C.Y. Qiu, L. Li, L.L. Hao, J.G. Wang, X. Zhou, Y.L. Kang, Effect of continuous annealing temperature on microstructure and properties of ferritic rolled interstitial-free steel, Int. J. Miner. Met. Mater. 25 (5) (2018) 536–546.
[7] P. Ghosh, C. Ghosh, R.K. Ray, D. Bhattacharjee, Precipitation behavior and texture formation at different stages of processing in an interstitial free high strength steel, Scr. Mater. 59 (3) (2008) 276–278.
[8] P. Ghosh, C. Ghosh, R.K. Ray, Thermodynamics of precipitation and textural development in batch-annealed interstitial-free high-strength steels, Acta Mater. 58 (11) (2010) 3842–3850.
[9] P. Ghosh, R.K. Ray, C. Ghosh, D. Bhattacharjee, Comparative study of precipitation behavior and texture formation in continuously annealed Ti and Ti+ Nb added interstitial-free high-strength steels, Scr. Mater. 58 (11) (2008) 939–942.
[10] W.C. Jeong, Role of aluminum in hot-rolled ultra-low-carbon Nb-interstitial-free steels, Metall. Mater. Trans. A 37 (12) (2006) 3737–3739.
[11] H. Kang, C.I. Garcia, K. Chin, A.J. Deardo, Effect of aluminum content on the mechanical properties of dual stabilized Ti–Nb interstitial free high strength steel (IF-HSS), ISIJ Int. 47 (3) (2007) 486–492.
[12] D.W. Beardsmore, J.Q. da Fonseca, J. Romero, C.A. English, S. R. Ortner, J. Sharples, A.H. Sherry, M.A. Wilkes, Study of Lüders phenomena in reactor pressure vessel steels, Mater. Sci. Eng. A 588 (2013) 151–166.
[13] D. Akama, N. Nakada, T. Tsuchiyama, S. Takaki, A. Hironaka, Discontinuous yielding induced by the addition of nickel to interstitial-free steel, Scr. Mater. 82 (2014) 13–16.
[14] S. Gao, A. Shibata, M. Chen, N. Park, N. Tsuji, Correlation between continuous/discontinuous yielding and Hall–Petch slope in high purity iron, Mater. Trans. 55 (1) (2014) 69–72.
[15] J. Zhang, Y. Cao, G. Jiang, H. Di, Effect of annealing temperature on the precipitation behavior and texture evolution in a warm-rolled P-containing interstitial-free high strength steel, Acta Metall. Sin. (Engl. Lett.) 27 (3) (2014) 395–400.
[16] W. Wang, R. Xu, Y. Hao, Q. Wang, L. Yu, Q. Che, et al., Corrosion fatigue behavior of friction stir processed interstitial free steel, J. Mater. Sci. Technol. 34 (1) (2018) 148–156.
[17] S.S. Sahay, B.H. Kumar, S.J. Krishnan, Microstructure evolution during batch annealing, J. Mater. Eng. Perform. 12 (6) (2003) 701–707.
[18] S.S. Sahay, A.M. Kumar, A. Chatterjee, Development of integrated model for batch annealing of cold rolled steels, Ironmak. Steelmak. 31 (2) (2004) 144–152.
[19] K. Banerjee, Physical metallurgy and drawability of extra deep drawing and interstitial free steels, in: Recrystallization, InTech, 2012.
[20] J. Shi, D. Cui, On optimizing batch annealing for the production of IF steels, Mater. Manuf. Process. 18 (1) (2003) 51–66.
[21] G. Anand, A. Sinha, P.P. Chattopadhyay, On the plasticity of interstitial-free steel subjected to cryogenic rolling followed by annealing, Mater. Manuf. Process. 28 (3) (2013) 242–248.
[22] B.J. Duggan, Y.Y. Tse, G. Lam, M.Z. Quadir, Deformation and recrystallization of interstitial free (IF) steel, Mater. Manuf. Process. 26 (1) (2011) 51–57.
[23] P.F. Wang, Z. Han, K. Lu, Enhanced tribological performance of a gradient nanostructured interstitial-free steel, Wear 402 (2018) 100–108.
[24] N.D. Sardinha, I.C. Santos, B.V. Andrade, R.A. Botelho, R.V. Oliveira, S.B. Diniz, A.D. Paula, L.P. Brandao, Mechanical properties and crystallographic texture of symmetrical and asymmetrical cold rolled IF steels, Mater. Res. 19 (5) (2016) 1042–1048.

[25] R. Yoda, I. Tsukatani, T. Inoue, T. Saito, Effect of chemical composition on recrystallization behavior and *r*-value in Ti-added ultra low carbon sheet steel, ISIJ Int. 34 (1) (1994) 70–76.
[26] R.K. Ray, P. Ghosh, An overview on precipitation and texture formation in IF and IFHS steels during processing, Mater. Manuf. Process. 25 (1–3) (2010) 195–201.
[27] M.A. Altuna, A. Iza-Mendia, I. Gutiérrez, Precipitation of Nb in ferrite after austenite conditioning. Part II: strengthening contribution in high-strength low-alloy (HSLA) steels, Metall. Mater. Trans. A 43 (12) (2012) 4571–4580.
[28] Y. Tanaka, T. Urabe, Y. Nagataki, A new type of high strength steel for exposed panels-high-strength steel with excellent formability, superior surface precision after press forming, and uniform surface appearance, JFE Tech. Rep. 4 (4) (2004) 17–27.
[29] P. Ghosh, R.K. Ray, B. Bhattacharya, S. Bhargava, Precipitation and texture formation in two cold rolled and batch annealed interstitial-free high strength steels, Scri. Mater. 55 (3) (2006) 271–274.
[30] R.K. Ray, A. Haldar, Texture development in extra low carbon (ELC) and interstitial free (IF) steels during warm rolling, Mater. Manuf. Process. 17 (5) (2002) 715–729.
[31] D. Llewellyn, R. Hudd, Steels: Metallurgy and Applications, Elsevier, 1998.
[32] R. Rana, S.B. Singh, Automotive Steels: Design, Metallurgy, Processing and Applications, Woodhead Publishing, 2016.
[33] R. Saha, R.K. Ray, D. Bhattacharjee, Attaining deep drawability and non-earing properties in Ti+ Nb interstitial-free steels through double cold rolling and annealing, Scr. Mater. 57 (3) (2007) 257–260.
[34] G. Bhargava, L. Patra, S. Pai, D. Mishra, A study on microstructure, texture and precipitation evolution at different stages of steel processing in interstitial free high strength steels, Trans. Indian Inst. Met. 70 (3) (2017) 631–637.
[35] P. Ghosh, R.K. Ray, Deep drawable steels, in: Automotive Steels, 2017, 113–143.
[36] A.H. Cottrell, B.A. Bilby, Dislocation theory of yielding and strain ageing of iron, Proc. Phys. Soc. A 62 (1) (1949) 49.